

# Numerical modelling of the hydrodynamic response of a fixed dual-chamber Oscillating Water Column Wave Energy Converter through the meshless DualSPHysics method

Gael ANASTAS<sup>a,1</sup>, João Alfredo SANTOS<sup>b</sup> and Conceição Juana E.M. FORTES<sup>a</sup>

<sup>a</sup>*Laboratorio Nacional de Engenharia Civil, LNEC*

<sup>b</sup>*Instituto Superior de Engenharia de Lisboa, ISEL, Centre for Marine Technology and Ocean Engineering, CENTEC*

**Abstract.** A numerical model of a dual-chamber Oscillating Water Columns (OWC) Wave Energy Converter (WEC) is built through the DualSPHysics software. This code is based on the Smoothed Particle Hydrodynamics (SPH) model, a Lagrangian meshless method where particles represent the flow, interact with structures, and exhibit large deformation with moving boundaries. A one phase approach – only water - is chosen in order to limit the computing time, as it increases with the total number of particles. The power take-off (PTO) of the system is modeled by the force applied by a vertical linear spring link on a floating plate inside the chamber. The force formula and coefficients are described, discussed, and tuned for various wave states to optimize the model. Validations against experimental data available from previous tests in wave flumes are performed. The floating plate heave of the numerical model is compared with the experimental free surface elevation. The result analyses establish the benefits and limits of DualSPHysics to model a fixed dual-chamber OWC WEC.

**Keywords.** Dual-chamber OWC, DualSPHysics, meshless method, PTO

## 1. Introduction

For decades it has been ascertained that the energy carried by ocean wind waves can be used to drive devices that convert it into clean electric energy. Depending on their type, design, and location with respect to the coast, a great diversity of technologies has been and is being developed to extract the ocean wave energy for conversion into electricity. The most common devices are referred to as the oscillating water column (OWC), hinged contour device, buoyant moored device, hinged flap, and overtopping device. The idea of combining breakwaters with OWC wave energy converters (WEC) emerged from an Indian wave energy program in 1996 [1]. The OWC wave energy device basically consists of an air turbine installed at the upper outlet of a partially submerged chamber. The waves propagate into the chamber through the submerged lip wall opening. During

---

<sup>1</sup> Gael Anastas, France; E-mail: [gael.anastas@mailden.net](mailto:gael.anastas@mailden.net); ganastas@lnec.pt

the presence of a wave crest, the air column is pushed upwards through the duct and drives the turbine to generate electricity. Although, when the wave troughs enter inside the chamber, the air column is pushed down. Hence, the pressure variations in the OWC chamber create a bidirectional air flow across a specific turbine, which rotates in a single way for both flow directions. Some of the attractive properties of OWC devices are attributed to the use of an air turbine as machinery because it is the single moving part, it is not in contact with the water, and provides an inherent energy storage by the inertia moment of the spinning shaft. Several OWC devices have been deployed all around the world, such as a breakwater equipped with an OWC plant was finished with a 40 kW Wells turbine in the Sea of Japan [2]. Another plant has been installed at the Pico Island (Azores, Portugal), equipped with a 400kW horizontal-axis Wells turbine-generator set rated at 400kW [3]. Some improvements in terms of design are being investigated to enhance the device hydrodynamic performance. For instance, the U-OWC concept has been installed in a full operative plant in Italy in 2016 [4]. More recently, the benefits of a proper dimensioned front step installation, and of the presence of two interconnected chambers have been described in [5] and [6]. OWC WEC are generally mimicked and analysed through mesh based CFD models ([7],[8]). Despite being very robust mathematically and computationally, mesh-based methods face important obstacles when capturing the free surface and non-linearities. For its expected capacity to overcome those challenges, the meshless CFD method approach has raised attention during the last years. Among various algorithms, the smoothed particle hydrodynamics (SPH) method is one of the most widely used. In the current research a one-phase 2D dual-chamber OWC model is built-up, based on the DualSPHysics code [9]. In addition, the turbine PTO damping force is computed using the Project Chrono solver and adapting the methodology detailed in [10]. The data used to validate the numerical model were sourced from the experimental tests of the OWC-Harbour project (PTDC/EME-REN/30866/2017), carried out in the wave flume of the Laboratório Nacional de Engenharia Civil (LNEC). This paper includes an overview of the OWC-Harbour project experimental campaign (section 2), along with a brief description of DualSPHysics code and Chrono project (section 3.a, 3.b). The modelling methodology is then explained (section 3.c, 3d), followed by the result presentation and assessment (section 4). Eventually (section 5), the relevance of the methodology is discussed.

## **2. Experimental Campaign**

The experimental tests were carried out in one of LNEC's irregular wave flumes. This flume is provided with a wave paddle, mounted on a horizontal electric-driven piston, capable of generating a variety of regular and irregular waves over a wide range of wave heights and periods. The flume is about 30 meters long. Its width varies from 1m, near the wave maker to 0.63m next to the model. This peculiar geometry allows the absorption of a fraction of the reflected wave energy, and partially offsets the lack of an Active Wave Absorption System (AWAS). The wave flume is provided with a passive absorption beach at the other end. The bottom level is not flat to adjust the water depth in front of the model entrance. The dual-chamber OWC device design (Figure 1) has been previously optimized according to the most frequent wave states at Madalena harbour surroundings (Azores – Portugal). Additionally, it is provided with a step at its entrance, improving the hydrodynamic performances as demonstrated in [7]. The model scale is 1:25 and the incident wave characteristics have been determined through the

Froude scaling method. The Free Surface Elevations (FSE) inside each chamber is monitored thanks to two ultrasonic sensors and one capacitive sensor. In addition, one digital pressure sensor ( $\pm 10\text{mBar}$ ) is connected to each air chamber. Seven resistive Wave Gauges (WG) are consciously distributed along the wave flume to characterise the incident waves on the OWC device thanks to the reflexion analysis.

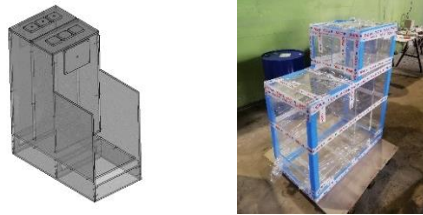


**Figure 1** Dual-Chamber OWC model

For OWC devices, an impulse turbine is commonly described as a nonlinear PTO [11], modelled, for small scales, thanks to an orifice [12], due to its simplicity and its well representative relation between pressure drop and flowrate. Here, the impulse turbine is modelled through a circular orifice of  $9\text{cm}^2$  (about 8% of the chamber horizontal area) at the upper part of

each chamber. Regular waves of 4cm height are generated with a water depth of 38,4cm in front of the model. The period range is 1.6s to 3s with a 0,2s increment.

### 3. Numerical Modelling

The novelty of this study comes from the choice of modelling the OWC dual-chamber device through the Lagrangian mesh-less based method DualSPHysics v5.0. This method has been used in an expanding range of applications within the field of Computation Fluid Dynamics (CFD), but rarely for OWC WEC application [10], and never for dual chamber OWC devices. The DualSPHysics code originates from the open source SPH model SPHysics. Although SPHysics allows problems to be simulated using high resolution and a wide range of formulations, the main problem for its application to real engineering problems is the excessively long computational run-times. Those drawbacks have been overcome by adding the option of using the parallel power computing of GPUs to the SPH methods, where the same loops for each particle during the simulation can be parallelized. The present work takes advantage of this improvement. Furthermore, the development of a one-phase model required an unusual way of computing the PTO damping effects inside the chambers. Fortunately, DualSPHysics code has been coupled with the Project Chrono solver. Chrono is a physics-based modelling and simulation infrastructure based on a platform-independent open-source design implemented in C++. This library can be embedded in a software project. The present paper implements a self-modified and re-compiled Chrono-4-0-0 library as described in Section 3.2. With a view to save computational time, it has been decided to develop a 2D model instead of 3D. This choice is validated by the experimental data. Indeed, the FSE measurements inside the chambers showed a symmetric behavior in the vertical longitudinal flume plane.

#### 3.1. Chrono code integration

DualSPHysics allows the use of the Project Chrono multi-body solver to compute rigid body constraints and collision detection [13]. It enables the possibility of using a set of bodies described in meshes, specifying restrictions applied to the bodies and computing

interactions between bodies, in a similar fashion to the Discrete Element Method implementation, but in a more stable manner. Once quantities from the rigid bodies are computed by DualSPHysics, the time step along with the linear and angular accelerations from each body, computed solely from fluid-body interaction, are sent to the Project Chrono module. For that time step, Chrono returns the linear and angular velocities, as well as the position, computed by integrating the fluid contributions with the dynamic or kinematic restrictions of the system, including collisions. The Chrono computing time isn't affected by the model particle total number.

### 3.2. PTO Damping Modelling

In this 2D numerical model, each chamber has a 4cm thick floating plate with a length of about 70% of the chamber length and a 50% density (Figure 2). Only the heave displacement is allowed. Each plate is connected to the fixed bottom through a solid-solid interaction computed by the Chrono code. This library proposes a wide range of interaction force formulations.

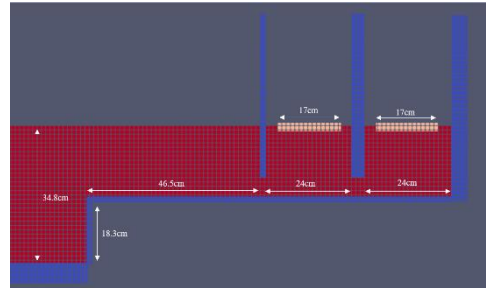


Figure 2 DualSPHysics OWC model: red-fluid/blue-walls/beige-plates

One of them is defined as a combination of a spring force with a coulomb damping force applied to a moving body:

$$F = -kx - c\dot{x} \quad (1)$$

where  $k$  is the stiffness,  $c$  the damping coefficient and  $x$  the body displacement. In [14], the authors numerically simulate the pressure drop due to the impulse turbine PTO damping absorption with the following equation:

$$p(t) = \frac{\rho_a}{2} \left( \frac{1}{c_d a} \right)^2 Q(t)^2 \text{sign}(Q) \quad (2)$$

with  $\rho_a$  the air density  $1,1225 \text{ kg/m}^3$ ,  $a$  the orifice area in  $\text{m}^2$ ,  $c_d$  an effective area dimensionless coefficient, and  $Q$  being the air flux,

$$Q(t) = v_{az}(t)S_c \quad (3)$$

where  $v_{az}(t)$  is the vertical air velocity and  $S_c$  the chamber area. The air compressibility effects are considered not relevant for the current model scale (1/25), as rigorously demonstrated in [15]. Consequently, inside the chamber, the vertical air flux is equal to the vertical water flux. Thus,  $v_{az}(t)$  is equal to the fluid vertical velocity inside the chamber  $v_z(t)$  assimilated to the plate heave displacement computed by SPH code. The force to apply to the numerical model plates is deduced from the pressure  $p(t)$ :

$$F(t) = -p(t)S_p \quad (4)$$

where  $S_p$  is the 2D horizontal plate area. Therefore,

$$F(t) = -S_p \left[ \frac{S_c v_z(t)}{c_d a} \right]^2 \frac{\rho_a}{2} \text{sign}(v_z) \quad (5)$$

$c_d$  value must be determined and depends on both orifice and air chamber geometries. In the present study the optimized value of 0,58 is set. Eq. (1) has been replaced by Eq. (5) in the Chrono-4-0-0 code. The library has been then recompiled on Ubuntu 18.04 (Linux

distribution) with gcc/g++4.9 and copied inside the DualSPHysics Library folder. In this way, the solid-solid interaction force between each floating plate and the fixed bottom is computed with Eq. (5) to simulate the impulse turbine PTO damping.

### 3.3. Configuration & Calibration

The computation time of each simulation step is directly related to the particle total number; therefore, the numerical flume length is shortened to 12.89m, picturing the flat flume bottom portion, and representing at least four wave lengths. Furthermore, the inter-particle distance ( $dp$ ) is set to 0.004m which represents a tenth of the wave height ( $H/10$ ). This is the minimum ratio recommended by the DualSPHysics developers.  $H/12$  and  $H/15$  have been tested in a convergence study without bringing accuracy refinement. The wave flume is composed of about 390000 fluid particles. The passive absorption beach is not modeled, however an AWAS is implemented. It has been confirmed that the wave generation isn't affected by the aforementioned discrepancies with reality. The wave generation convergence has been confirmed by comparing numerical and experimental FSE along the flume and it concluded on the reliable numerical replication of the generated waves. The plate length (70% of the chamber length) is large enough to prevent the water particles to jump above the plate and short enough to avoid any interaction between the plate and the OWC walls. The plate density has been selected by generating waves without and with various densities' plates without applying PTO forces. A 50% density plate appears to be the most adapted to replicate the FSE heave displacement inside the chambers. An NVIDIA Quadro P2200 GPU is implemented to accelerate the calculation runtime. Eventually, it takes 47min to simulate 10s.

## Results and validation

Numerical simulations have been conducted generating regular waves of 4cm height and periods ranging from 1.6 to 3s with a 0,2s increment. The free surface elevation at the center of each chamber is extracted from the simulation outputs and compared to the capacitive gauge measurements. Here, only two cases are presented in diagrams (Figure 3 & 4), however, Table 1 presents for all cases, the Root Mean Square Error (RMSE) and the normalized maximum heave displacement error (NRH) calculated with Eq. (6).

$$NRH = \frac{\widehat{h}_i - \widehat{h}_j}{\widehat{h}_i} \quad (6)$$

where  $\widehat{h}_i$  and  $\widehat{h}_j$  are the average of the maximum heave motion on each sinusoid period for, respectively, the experimental and the model FSE values.

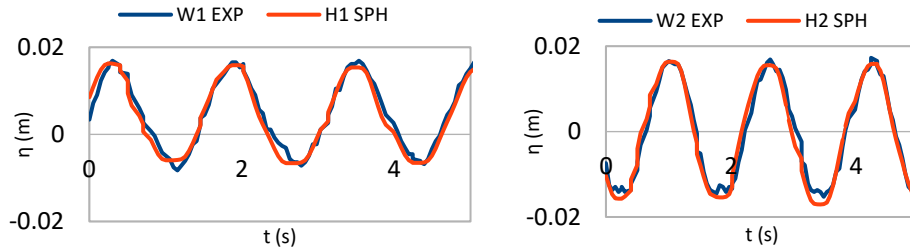


**Figure 3** Free-surface elevation at the center of chamber 1 (left) and chamber 2 (right) for  $T = 1.6s$

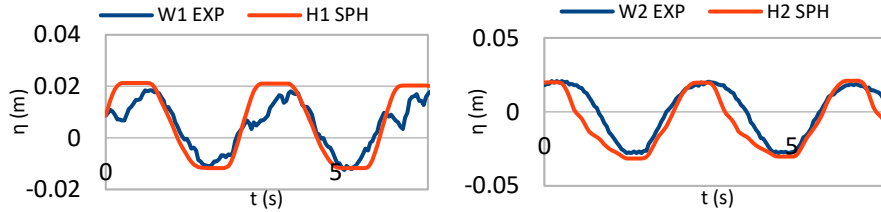


**Figure 4** Free-surface elevation at the center of chamber 1 (left) and chamber 2 (right) for  $T = 3$  s

As expected, and confirmed during the experimental campaign, vortex fluid motions materialize at both front and middle OWC wall immersed edges. The DualSPHysics mesh-less model has been able to replicate this fluid behavior (Figure 5). Some slight turbulences can be seen at the front step upper corner, such behavior being also confirmed by the experimental tests.

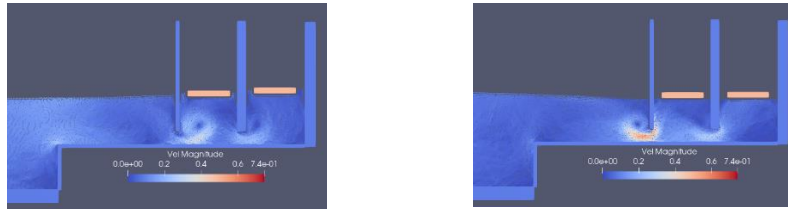


**Figure 5** Particle velocity magnitudes in the device vicinity for  $H=4$ cm and  $T=2.4$ s

Furthermore, Figures 3 and 4 show the two types of resonant responses that may occur inside the chambers, on one hand the piston-type resonance, where the FSE stays almost flat and its heave oscillation is regular (Figure 3), and on the other hand the sloshing-type resonances, where complex energy dissipative non-linear behaviors happen, as in chamber 1 for  $T=3.0$ s (Figure 4). This last resonance response, where the wave inside the chamber is reflected by the rear wall and propagates to the front part, appears mostly in cases of short incoming wave lengths ( $\lambda$ ) compared to the chamber width ( $W_{\text{chamber}}/\lambda > 0.1$ ). Usually, OWC designs try to avoid this chaotic performance, however this occurrence is not uncommon. In the current study configuration  $W_{\text{chamber}}/\lambda_{\text{max}} = 0.025$ , however the sloshing effects are present with variable intensities and exclusively in the first chamber, in all cases where  $T$  is equal to or larger than 1.8s. Indeed, the second chamber always shows a more linear behavior, similar to the piston-type motion, due to the first chamber energy absorption. Unfortunately, the numerical method described in this paper cannot replicate the effects of the fluid sloshing inside the chamber. Primarily, because of the plate motion constraints on the down below particles, and secondly, because the paradigm of the PTO force definition (Eq. (5)) considers an ideal FSE piston-type motion inside the chambers. Regarding the RMSE values (Table 1), the overall accuracy of the model is high, with all values under 1% for both chambers and better results for chamber 2 in general, as expected from its more linear behavior. The comparison of the maximum heave motion (NRH) is also giving acceptable results with an error inferior to 10%. In most cases the heave motion is overestimated, corresponding to positive values of NRH, mainly because of the model non-integration of the dissipation effects due to sloshing. The water column vertical motion is commonly described as a single degree of freedom system of an effective mass composed by the water trapped inside the chamber and an added mass. The natural frequency is affected

by this mass value and by the restoring force due to gravity, thus the plate introduction in the numerical model may lead to a substantial modification on the device hydrodynamic response for some of the excitation configurations, as for  $T=1.8s$  and  $2.2s$ , where the NRH exceed 25% (Table 1). A small period deviation has been detected for those cases.

**Table 1.** RMSE and RH with wave height  $H = 4cm$  and  $T = [1.6-3s]$  for chamber 1 and 2

T (s)	Chamber 1		Chamber 2	
	RMSE (%)	NRH (%)	RMSE (%)	NRH (%)
1.6	0.18	8.5	0.17	0.43
1.8	0.25	21.4	0.25	6.4
2	0.79	2.65	0.35	2.43
2.2	0.51	27.5	0.29	5.35
2.4	0.68	5.33	0.35	1.63
2.6	0.5	7.97	0.54	2.05
2.8	0.67	6.48	0.7	5.39
3	0.62	5.25	0.853	4.43

More effects due to the plate presence must be pointed out, especially in chamber 2 for the higher wave periods, where the vertical oscillation from experiment is still smooth and linear, but for which the numerical model FSE descending phase is accelerated, leading to an asymmetric motion with both convex and concave shapes (Figure 4), certainly due to discrepancies in the restoring force amplitude. Furthermore, the 2D modeling is, as well, a source of disparity with reality. Indeed, the three-dimensional wave field distribution around the chamber consistently affects the hydrodynamic performance of the device. Eventually, during the experimental campaign, the existence of a 5cm gap between the external model wall and the internal flume wall on both sides, allowed a part of the incoming wave to pass behind the model. A portion of these waves is trapped between the back of the model and the passive absorption beach and is dissipated. Nevertheless, the rest comes back to the front model and interacts with the incoming waves leading to more dissimilarity with the field measurements.

#### 4. Conclusions

In this study, a one-phase numerical model of a dual-chamber OWC WEC device has been developed with DualSPHysics mesh-less method, disregarding the air compressibility effect. The numerical results of the free-surface elevation inside both chambers have been validated through experimental data comparison, obtained from the OWC-Harbour project experimental campaign. The impulse turbine PTO damping has been considered non-linear and modelled in DualSPHysics by adding a floating plate inside each chamber, on which a PTO force is implemented using the Project Chrono library. Results show that DualSPHysics can be considered a reliable tool for fixed OWC WEC modelling. However, the use of a one-phase solver limits the results accuracy as the model is not able replicate the sloshing-type motion occurring in the first chamber. The addition of a floating plate has also an impact on the model natural frequency leading to discrepancies with reality. It is expected that the numerical technique for estimating the chamber FSE can be improved by considering three-dimensional effects. Future research could also consider air compressibility to improve the model accuracy.

## Acknowledgments

This research has been supported by the FCT project “PTDC/EME-REN/30866/2017. Special thanks to the DualSPHysics development team, to Dr. Rezanejad and to Dr. Gadelho for their support. The authors declare no conflict of interest.

## References

- [1] Graw K.-U. 1996. Wave energy breakwaters - a device comparison”; Conference in Ocean Engineering, IIT Madras, India.
- [2] Masuda Y, McCormick ME. Experiences in pneumatic wave energy conversion in Japan. In Utilization of Ocean Waves—Wave to Energy Conversion; ASCE Library: Reston, VA, USA, 2015; pp. 1–33.
- [3] Falcão AFO, Sarmiento AJNA, Gato LMC, Brito-Melo A. The Pico OWC wave power plant: Its lifetime from conception to closure 1986–2018. *Applied Ocean Research*. 2020; 98, 102104. <https://doi.org/10.1016/j.apor.2020.102104>.
- [4] Arena F, Romolo A, Malara G, Fiamma V, Laface V. The first full operative U-OWC plants in the port of Civitavecchia. *Proceedings of the International Conference on Offshore Mechanics and Arctic Engineering – OMAE*. 2017; 10. <https://doi.org/10.1115/OMAE2017-62036>.
- [5] Rezanejad K, Gadelho, JFM, López I, Carballo R, Soares CG. Improving the hydrodynamic performance of owc wave energy converter by attaching a step. *Proceedings of the International Conference on Offshore Mechanics and Arctic Eng. – OMAE*. 2019; 10. <https://doi.org/10.1115/omae2019-96408>.
- [6] Rezanejad K, Bhattacharjee J, Guedes Soares C. Analytical and numerical study of dual-chamber oscillating water columns on stepped bottom. *Renewable Energy*. 2015; 75, 272–282. <https://doi.org/10.1016/j.renene.2014.09.050>.
- [7] Iturrioz A, Guanche R, Lara JL, Vidal C, Losada IJ. Validation of OpenFOAM® for Oscillating Water Column three-dimensional modeling. *Ocean Engineering*. (2015); 107, 222–236. <https://doi.org/10.1016/j.oceaneng.2015.07.051>
- [8] Rezanejad K, Gadelho JFM, Guedes Soares C. Hydrodynamic analysis of an oscillating water column wave energy converter in the stepped bottom condition using CFD. *Renew.E.*. 2019; 135, 1241–1259.
- [9] Crespo AJC, Domínguez JM, Rogers BD, Gómez-Gesteira M, Longshaw S, Canelas R, Vacondio R, Barreiro A, García-Feal O. DualSPHysics: Open-source parallel CFD solver based on Smoothed Particle Hydrodynamics (SPH). *Computer Physics Communications*. 2015; 187, 204–216. <https://doi.org/10.1016/j.cpc.2014.10.004>.
- [10] Quartier N, Crespo AJC, Domínguez JM, Stratigaki V, Troch P. Efficient response of an onshore Oscillating Water Column Wave Energy Converter using a one-phase SPH model coupled with a multiphysics library. *Applied Ocean Research*. 2021; 115. <https://doi.org/10.1016/j.apor.2021.102856>.
- [11] Anand S, Jayashankar V, Nagata S., Toyota K, Takao M, Setoguchi T. Performance estimation of bi-directional turbines in wave energy plants. *Journal of Thermal Science*. 2007; 16(4): 346–352.
- [12] Stappenbelt B, Cooper P, Fiorentini M. Prediction of the heave response of a floating oscillating water column wave energy converter. *Proc. 9<sup>th</sup> Eur. Wave Tidal Engy. Conf.*, Southampton, UK, 5-9th Sep. 2011.
- [13] Tasora A, Serban R, Mazhar H, Pazouki A, Melanz D, Fleischmann J, Taylor M, Sugiyama H, Negrut D. Chrono: An open source multi-physics dynamics engine. In Kozubek T, Blaheta R, Šístek J, Rozložník M, Čermák M, editors. *High Performance Computing in Science and Engineering – Lecture Notes in Computer Science*. Springer; 2016: 19–49.
- [14] Bingham HB, Ducasse D, Nielsen K, Read R. Hydrodynamic analysis of oscillating water column wave energy devices. *J. of Ocean Eng.. Marine Ener.* 2015); 1(4). <https://doi.org/10.1007/s40722-015-0032-4>.
- [15] Falcão AFO, Henriques JCC. Model-prototype similarity of oscillating-water-column wave energy converters. *Int J Mar Energy*. 2014; 6:18–3